Polaron resonances in two vertically stacked quantum dots

Paweł Karwat,* Krzysztof Gawarecki, and Paweł Machnikowski
Department of Theoretical Physics, Faculty of Fundamental Problems of Technology, Wrocław University of Science and Technology, 50-370 Wrocław, Poland
(Received 26 January 2017; revised manuscript received 12 April 2017; published 13 June 2017)

In this work, we present a theoretical study of polaron states in a double-quantum-dot system. We present realistic calculations which combine 8-band $\boldsymbol{k}\cdot\boldsymbol{p}$ model, configuration-interaction approach, and collective-modes method. We investigate the dependence of polaron energy branches on axial electric field. We show that coupling between carriers and longitudinal optical phonons via Fröhlich interaction leads to qualitative and quantitative reconstruction of the optical spectra. In particular, we study the structure of resonances between the states localized in different dots. We show that p-shell states are strongly coupled to the phonon replicas of s-shell states, in contrast to the weak direct s-p coupling. We discuss also the dependence of the phonon-assisted tunnel coupling strength on the separation between the dots.

DOI: 10.1103/PhysRevB.95.235421

I. INTRODUCTION

Self-assembled quantum dots (QDs) are continuously attracting attention both in fundamental research, as well as in the development of novel applications in quantum optics and quantum information. With the continuing effort and progress in miniaturization, QDs find technological use in many types of devices, including QD lasers [1,2], solar cells [3], and many others.

One of the most interesting aspects of QD physics is related to carrier-phonon coupling. Apart from dissipative processes induced by phonons, this coupling can lead to the formation of polarons, that is, eigenstates of the interacting carrier-phonon systems in which the carrier state is correlated with the coherent field of longitudinal optical (LO) phonons. In QDs, the carrier spectrum is discrete, while the relatively weak carrier localization limits the effectively coupled LO phonons to the nearly dispersionless zone-center part of their spectrum. As a result, the system is in the strong coupling regime and the polaron states are manifested in the form of pronounced resonances whenever one excited state spectrally crosses a LO-phonon replica of another state [4–6]. The width of the resonances provides a natural quantitative measure of the strength of the carrier-phonon coupling. The effectively dispersionless nature of LO phonons forming the polaron states in QDs makes it possible to describe the system in terms of a finite number of collective modes [7], which opens the path to numerically exact diagonalization of the carrier-LO-phonon (Fröhlich) Hamiltonian in a restricted basis of carrier states. Experimental and theoretical work on QD polarons has brought good understanding of their essential properties both for single-electron states and for excitons [8,9], as well as of their crucial role for carrier relaxation in self-assembled QD systems, where typical energy level separations are comparable to the LO-phonon energy [10–14].

Systems composed of vertically stacked coupled QDs offer richer physical properties and a higher level of controllability than a single QD. In particular, a double-quantum-dot (DQD) structure supports spatially direct and indirect states with different dipole moments, the energy of which can be tuned in a broad range by applying an axial electric field [15–19]. Recently, the spectrum of such a system was mapped out by combined spectroscopy techniques and successfully modeled using 8-band $\boldsymbol{k}\cdot\boldsymbol{p}$ theory in the envelope-function approximation [20]. The electric-field tunability of energy levels in such systems might allow one to study the polaron resonances as a function of the electric field by matching various energy shells of the two dots, which offers much more flexibility in comparison to the single-QD studies, where only limited tunability by magnetic field is available [4,5].

In this paper, we study polaron states in a DQD structure. In such a coupled structure, a prerequisite of any quantitatively reasonable modeling is an accurate model of wave functions. Therefore, in order to find electron and hole states we apply the 8-band $\boldsymbol{k}\cdot\boldsymbol{p}$ model with strain distribution found within continuous elasticity approach [21]. We then calculate exciton states using the configuration-interaction method. Finally, polaron states are found by orthogonalization of the Fröhlich Hamiltonian in the basis of collective phonon modes [7]. We propose a numerically efficient scheme of mode orthogonalization and selection of effectively coupled modes based on the Rowe orthogonalization [22]. We study the system spectrum, focusing on the polaron resonances, i.e., the spectral anticrossing structures appearing when the energies of two carrier states differ by one LO-phonon energy. We show that the width of such a LO-phonon-assisted resonance between direct and indirect exciton states of the same symmetry follows an exponential dependence on the interdot separation with a similar exponent but lower amplitude, as compared to the direct resonance. In contrast, for a pair of states with different symmetry, where the direct resonance is only allowed by weak spin-orbit effects, the coupling mediated by LO phonons is much stronger than the direct one.

The paper is organized as follows. In Sec. II, we define the system under consideration and the theoretical model. Next, in Sec. III we present the results. Section IV contains the final discussion. In the Appendix, we justify the basis cutoff used in our calculations.

II. MODEL AND NUMERICAL METHOD

In this section, we first describe the carrier system and its model used in our calculations and summarize the essential

*pawel.karwat@pwr.edu.pl

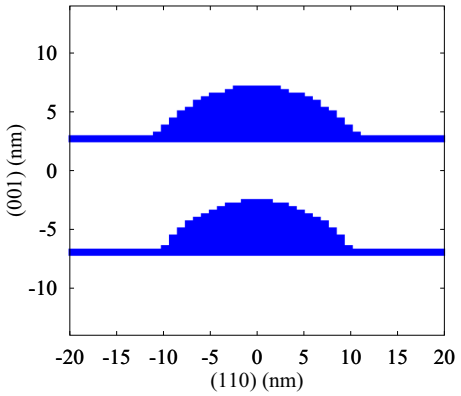

FIG. 1. Material distribution in the system.

features of the exciton spectrum to facilitate further discussion of the polaronic effects (Sec. II A). Next, we define the LO-phonon-related part of the model (Sec. II B). Then, we present the collective mode method with the mode orthogonalization scheme (Sec. II C).

A. Carrier system and its model

The system under study is made up of two vertically stacked InGaAs/GaAs self-assembled QDs resting on wetting layers. We assume lens shape of the upper (u) and lower (l) dot. In our calculations, we take height $h = 4.2$ nm (the same for both dots) and base radii $r_\mathrm{l} = 10.2$ nm, $r_\mathrm{u} = 10.8$ nm. The local InAs content in each QD and in the wetting layers is 80% InAs, the matrix contains 100% GaAs. The cross section of the InGaAs distribution is shown in Fig. 1.

The Hamiltonian of a system of carriers coupled to LO phonons is

$$H = H_0 + V_\mathrm{c} + V_\mathrm{ef} + H_\mathrm{ph} + H_\mathrm{F},$$

where H_0 describes the single-particle states, V_c is the Coulomb interaction between the particles, V_ef represents an axial electric field, H_ph is the Hamiltonian of the LO-phonon bath, and H_F is a Fröhlich interaction between carriers and LO phonons.

The first term of the Hamiltonian is

$$H_0 = \sum_n \epsilon_n^{(e)} a_n^\dagger a_n + \sum_m \epsilon_m^{(h)} h_m^\dagger h_m,$$

where $\epsilon_n^{(e)}/\epsilon_m^{(h)}$ are the energies of the electron/hole states obtained from the 8-band $\boldsymbol{k}\cdot\boldsymbol{p}$ calculations, $a_n^\dagger/h_m^\dagger$, a_n/h_m are the creation and annihilation operators of the electron/hole in the state n/m, respectively.

The Coulomb interaction is

$$V_\mathrm{c} = \sum_{nn'mm'} v_{nmm'n'} a_n^\dagger h_m^\dagger h_{m'} a_{n'},$$

where

$$v_{nmm'n'} = -\frac{e^2}{4\pi\epsilon_0\epsilon_\infty} \int d\boldsymbol{r} \int d\boldsymbol{r}' \Psi_n^{*(e)}(\boldsymbol{r}) \Psi_m^{*(h)}(\boldsymbol{r}') \times \frac{1}{|\boldsymbol{r}-\boldsymbol{r}'|} \Psi_{m'}^{(h)}(\boldsymbol{r}') \Psi_{n'}^{(e)}(\boldsymbol{r}).$$

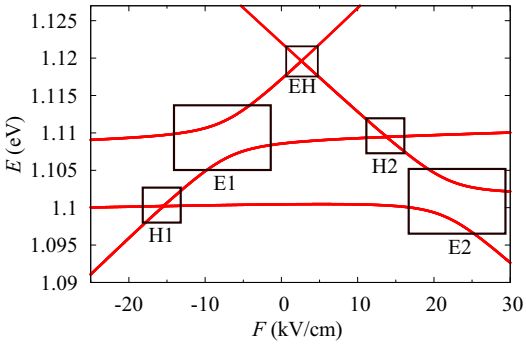

FIG. 2. Schematic plot of exciton energy branches as a function of external axial electric field at $D = 9$ nm.

Here, e is the electron charge, ϵ_0 and $\epsilon_\infty = 10.6$ are vacuum permittivity and high-frequency dielectric constant (we take GaAs values for dielectric constants [23]), $\Psi_n^{(e)}(\boldsymbol{r})/\Psi_m^{(h)}(\boldsymbol{r}')$ corresponds to the electron/hole wave functions which, according to our $\boldsymbol{k}\cdot\boldsymbol{p}$ model, are eight-component spinors. For the sake of efficiency, we calculate $v_{nmm'n'}$ in the inverse space (see details in Ref. [24]).

The potential of an axial electric field is defined by

$$V_\mathrm{ef} = \sum_{nn'} Z_{nn'}^{(e)} a_n^\dagger a_{n'} - \sum_{mm'} Z_{mm'}^{(h)} h_m^\dagger h_{m'},$$

where

$$Z_{ij}^{(e/h)} = F_z \int d\boldsymbol{r}\, \Psi_i^{*(e/h)}(\boldsymbol{r}) z \Psi_j^{(e/h)}(\boldsymbol{r})$$

and F_z is the magnitude of the electric field in the z direction.

The strain distribution in the system is taken into account within the standard continuous elasticity framework [21]. Piezoelectricity is included up to the second order in strain tensor elements [25] using parameters from Ref. [26]. In order to find electron and hole states, we perform the calculation using the 8-band $\boldsymbol{k}\cdot\boldsymbol{p}$ method in the envelope-function approximation. The calculation details have been widely described in Refs. [27,28] and material parameters are taken from Ref. [29].

Having the single-particle states, we then compute the exciton states which are found using the configuration-interaction (CI) method. The axial field is included at the CI stage [30]. Due to numerical efficiency reasons, we limit our basis to four lowest electron and hole states (i.e., electron and hole s shell in the lower and in the upper dots). A part of the exciton spectrum obtained in this way[1] is schematically presented in Fig. 2 (obtained by restricting the basis to s states only). This well-known spectrum of excitons in an electric field [15,16] is composed of spatially direct and indirect exciton states, clearly distinguishable by the small and large slopes of the field dependence of their energies, respectively. If two such states are tuned into the resonance (and if the symmetry of the states is such that selection rules are met), avoided crossing appears in the energy spectrum [15–19]. In Fig. 2,

[1]Since the LO-phonon coupling is not included explicitly in this calculation, we have replaced ϵ_∞ by ϵ_s in V_c to account for the LO-phonon-induced contribution to the screening.

these resonance structures are marked by E1, E2 (electron tunneling resonance), H1, H2 (hole tunneling), and EH (very weak coupling between two indirect configurations).

We stress that Fig. 2 is a schematic plot that shows only the electric-field dependence and general structure of resonances of s-shell states. In a full model, excited states would appear in the presented parameter window, forming a more complex pattern of tunnel and Coulomb resonances [20,24]. Another point is that even with a basis extended by adding higher electron and/or hole shells with respect to in-plane excitation, as is common in this kind of modeling, the wave function within a single QD remains rigid against shifts along the growth axis and the only degree of freedom is the transfer between the dots. This precludes the appearance of strong effects related to charge separation within a single QD in an axial electric field, that appear when the potential energy drop across the QD is comparable with the excitation energy for the relative motion [31]. However, for a strongly confined, self-assembled system with the F field along the axis of the strongest confinement and with field magnitudes on the order of 10 kV/cm, the system polarizability is negligible. Quantitatively, even for a very conservative choice of the excitation energy along the growth axis, the ratio of the two quantities mentioned above is on the order of at most 10^{-2}. Therefore, we are far below the field range where the effects described in Ref. [31] occur. This is in fact consistent with experiments, where the field-dependent spectra of QDs show an approximately uniform, weak slope of the direct exciton lines (attributed to the built-in, intra-QD dipole) throughout the investigated range of fields (see, e.g., Ref. [20]). In a double-QD system, the spectrum is clearly dominated by the transitions between spatially direct and indirect excitons, which are correctly described by our numerical model [20].

B. LO phonons

In the polaron formation, we assume nondispersive LO-phonon modes with $\hbar\Omega = 36$ meV. The LO-phonon bath is then described by the Hamiltonian

$$H_{\mathrm{ph}} = \sum_{\boldsymbol{q}} \hbar\Omega b^{\dagger}_{\boldsymbol{q}} b_{\boldsymbol{q}},$$

where $b^{\dagger}_{\boldsymbol{q}}$ and $b_{\boldsymbol{q}}$ are, respectively, the creation and annihilation operators for the LO-phonon mode $\boldsymbol{q}$. The carrier-phonon coupling is modeled by the Fröhlich Hamiltonian

$$H_{\mathrm{F}} = -\sum_{\boldsymbol{q}} \frac{e}{q}\sqrt{\frac{\hbar\Omega}{2V\widetilde{\epsilon}\epsilon_0}}\left(\sum_{nn'} \mathcal{F}^{(e)}_{nn'}(\boldsymbol{q}) a^{\dagger}_{n} a_{n'} - \sum_{mm'} \mathcal{F}^{(h)}_{mm'}(\boldsymbol{q}) h^{\dagger}_{m} h_{m'}\right)(b_{\boldsymbol{q}} + b^{\dagger}_{-\boldsymbol{q}}),$$

where $\widetilde{\epsilon} = (1/\epsilon_{\infty} - 1/\epsilon_s)^{-1}$, $\epsilon_s = 12.4$ is a static dielectric constant in GaAs, V is the normalization volume for phonon modes, and $\mathcal{F}^{(e/h)}_{nn'}(\boldsymbol{q}) = \mathcal{F}^{(e/h)*}_{n'n}(-\boldsymbol{q})$ is the one-particle (electron or hole) form factor

$$\mathcal{F}^{(e/h)}_{ij}(\boldsymbol{q}) = \int \Psi^{*(e/h)}_{i}(\boldsymbol{r})\Psi^{(e/h)}_{j}(\boldsymbol{r}) e^{i\boldsymbol{k}\cdot\boldsymbol{r}} d\boldsymbol{r}.$$

We perform calculations for excitonic polaron states in the basis of noninteracting electron and hole configurations $|\nu\rangle = |n\rangle_e \otimes |m\rangle_h$. In this pair-state basis the Fröhlich Hamiltonian for two-particle (exciton) states has the form

$$H_{\mathrm{F}} = -\sum_{\boldsymbol{q}} \frac{e}{q}\sqrt{\frac{\hbar\Omega}{2V\widetilde{\epsilon}\epsilon_0}} \sum_{\nu\nu'} \mathcal{F}^{(\mathrm{x})}_{\nu\nu'}(\boldsymbol{q}) |\nu\rangle\langle\nu'| (b_{\boldsymbol{q}} + b^{\dagger}_{-\boldsymbol{q}}), \quad (1)$$

where $\mathcal{F}^{(\mathrm{x})}_{\nu\nu'} = \mathcal{F}^{(e)}_{nn'}(\boldsymbol{q})\delta_{mm'} - \mathcal{F}^{(h)}_{mm'}(\boldsymbol{q})\delta_{nn'}$ with $\nu \sim (nm)$, $\nu' \sim (n'm')$.

C. Collective modes

The direct diagonalization of the Hamiltonian would imply sampling the $\boldsymbol{q}$ space, which is not feasible due to the large number of required $\boldsymbol{q}$ points. However, for nondispersive LO-phonon modes, one can use the collective modes method [7]. One defines the collective modes corresponding to the annihilation operators

$$\widetilde{B}_{\nu\mu} = \sum_{\boldsymbol{q}} \sqrt{\frac{l_0}{V}} \frac{1}{q} \mathcal{F}^{(\mathrm{x})}_{\nu\mu}(\boldsymbol{q}) b_{\boldsymbol{q}}, \quad (2)$$

where l_0 is an arbitrary characteristic length. The Fröhlich Hamiltonian then becomes

$$H_{\mathrm{F}} = -\sum_{\nu\mu} \sqrt{\frac{\hbar\Omega e^2}{2l_0\widetilde{\epsilon}\epsilon_0}} |\nu\rangle\langle\mu| \widetilde{B}_{\nu\mu} + \mathrm{H.c.} \quad (3)$$

However, the collective phonon modes $\widetilde{B}_{\nu\mu}$ are not orthonormal in the sense of canonical commutation relations. In order to simplify notation, in the following we will use a combined index j to represent the pair (ν,μ). Then, the commutator is

$$A_{j'j} = [\widetilde{B}_j, \widetilde{B}^{\dagger}_{j'}] = (\mathcal{F}_{j'}, \mathcal{F}_j), \quad (4)$$

where

$$(\mathcal{F}_{j'}, \mathcal{F}_j) = \frac{l_0}{V} \sum_{\boldsymbol{q}} \frac{1}{q^2} \mathcal{F}^{*}_{j'}(\boldsymbol{q}) \mathcal{F}_j(\boldsymbol{q}) \quad (5)$$

is the scalar product of the form factors, defined with an appropriate weight. Thus, canonical commutators between the new modes are related to the orthogonality of the form factors, which is not guaranteed in general.

At this point, one has to choose between the original approach involving orthogonalization of the modes [7] and the alternative method of nonorthogonal modes [32]. The latter saves one computational step required for orthogonalization but becomes inconvenient when the form factors defining the modes are not guaranteed to be linearly independent, which is the case, e.g., for the Fock-Darwin model [6]. Here, we use an efficient method of selecting a spanning set of orthogonal modes based on Löwdin's symmetric orthogonalization [33] in the form proposed by Rowe [22], in which the possible linear dependence of the modes is naturally taken into account.

Thus, following Rowe [22], if λ_α are the nonzero eigenvalues of the Hermitian, positive-semidefinite Gram matrix A [Eq. (4)] and $\boldsymbol{u}^{(\alpha)} = (u^{(\alpha)}_1, u^{(\alpha)}_2 \ldots)$ are the corresponding

normalized eigenvectors, then the functions

$$\mathcal{G}_\alpha(\boldsymbol{q}) = \frac{1}{\sqrt{\lambda_\alpha}} \sum_j u_j^{(\alpha)} \mathcal{F}_j(\boldsymbol{q})$$

are orthonormal. On the other hand, the set of form factors $\mathcal{F}_j$ satisfies a linear dependence relation $\sum_j u_j^{(\alpha)} \mathcal{F}_j = 0$ if and only if $\boldsymbol{u}^{(\alpha)}$ is in the kernel of A. For α such that $\lambda_\alpha \neq 0$, define the modes

$$B_\alpha = \sum_{\boldsymbol{q}} \sqrt{\frac{l_0}{V}} \frac{1}{q} \mathcal{G}_\alpha(\boldsymbol{q}) b_{\boldsymbol{q}}. \tag{6}$$

These modes are orthonormal, i.e., they satisfy the canonical commutation relations $[B_\alpha, B_{\alpha'}^\dagger] = \delta_{\alpha\alpha'}$, etc. On the other hand, completeness of the set $\{\boldsymbol{u}^{(\alpha)}\}$ implies that $\mathcal{F}_j(\boldsymbol{q}) = \sum_\alpha u_j^{(\alpha)*} \sqrt{\lambda_\alpha} \mathcal{G}_\alpha(\boldsymbol{q})$. Substituting this relation to Eq. (2) and using Eq. (6) one finds, returning to the original indexing ($j \to \nu,\mu$), $\widetilde{B}_{\nu\mu} = \sum_\alpha u_{\nu\mu}^{(\alpha)*} \sqrt{\lambda_\alpha} B_\alpha$, hence, the Fröhlich Hamiltonian [Eq. (3)] can be written in terms of the orthogonal modes in the form

$$H_{\mathrm{F}} = \sum_{\alpha\nu\mu} C_{\nu\mu}^{(\alpha)} B_\alpha |\nu\rangle\langle\mu| + \mathrm{H.c.}, \tag{7}$$

where the coupling coefficient reads as

$$C_{\nu\mu}^{(\alpha)} = \sqrt{\frac{\hbar\Omega e^2}{2 l_0 \widetilde{\epsilon} \epsilon_0}} \sqrt{\lambda_\alpha} u_{\nu\mu}^{(\alpha)*}.$$

Finally, we diagonalize this Hamiltonian in the space of zero-, one-, and two-phonon states

$$|\Psi_i\rangle = \sum_\nu d_\nu |\nu\rangle + \sum_{\nu\alpha} d_{\nu\alpha} B_\alpha^\dagger |\nu\rangle + \sum_{\nu\alpha\beta} d_{\nu\alpha\beta} \eta_{\alpha\beta} B_\alpha^\dagger B_\beta^\dagger |\nu\rangle.$$

Here, d_ν, $d_{\nu\alpha}$, and $d_{\nu\alpha\beta}$ are the coefficients of the zero-, one-, and two-phonon states, respectively, and ν corresponds to the noninteracting electron-hole pair states defined in Sec. II B, while $\eta_{\alpha\beta} = 1/\sqrt{2}$ for $\alpha = \beta$ and 1 otherwise. As a result of this procedure, for the exciton-polaron problem with a restricted exciton basis the Hamiltonian involves only a small number of orthogonal modes out of the initial n^2 modes, where n denotes number of exciton states.

Since the Hilbert space of the collective-mode model is infinite dimensional, a cutoff for the number of phonons is needed in the numerical calculations. Here, we include configurations up to two LO phonons. In order to validate this approximation we have calculated the spectrum around one of the resonances to be discussed in Sec. III using an extended, three-phonon basis. As shown in detail in the Appendix, including three-phonon configurations only slightly shifts the position of the main resonance and does not affect its width noticeably.

The fast convergence of the results with respect to the number of phonons in the model is consistent with the fact that InAs and GaAs are moderately polar materials. In addition, for the globally neutral excitonic states, partial charge cancellation reduces the Fröhlich coupling. The Huang-Rhys factor for the ground state

$$\xi = \frac{\sum_\alpha |C_{00}^{(\alpha)}|^2}{(\hbar\Omega)^2},$$

that is commonly used to quantify the strength of the polaronic effects, is only 5.15×10^{-3} in our case, which indicates that the system studied here is well within the perturbative regime and strong polaronic effects (that might require a nonperturbative adjustment of the computational basis) do not occur here.

III. RESULTS

The polaron energy branches were calculated as a function of an axial electric field (Fig. 3). As described in Sec. II, every polaron state $|\Psi_i\rangle$ is expressed in the basis of zero-, one-,

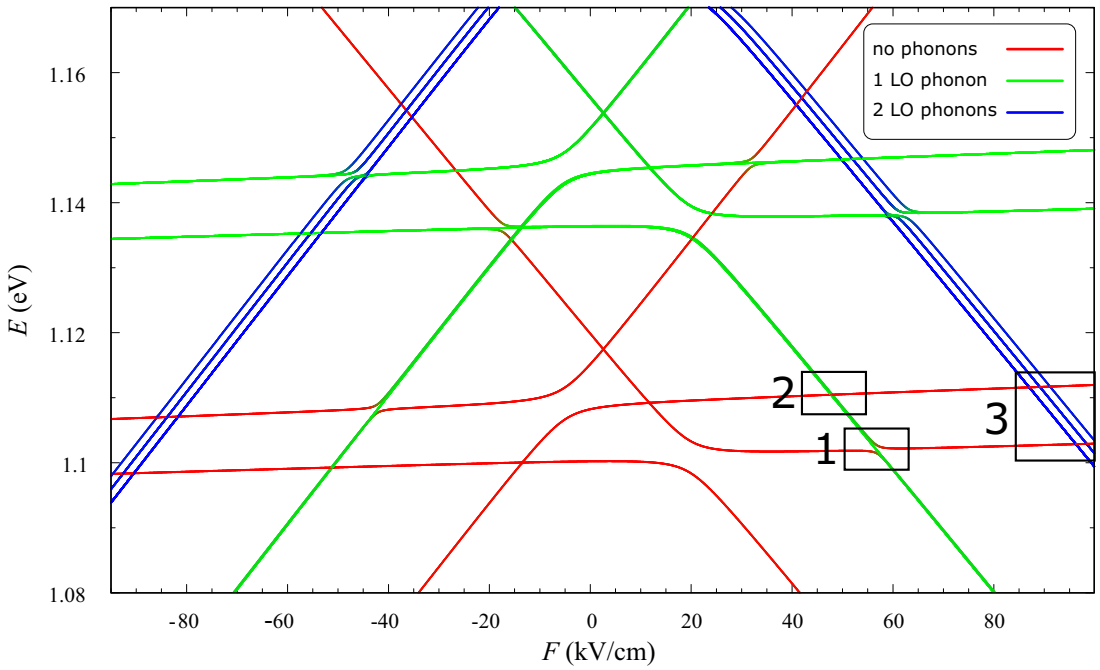

FIG. 3. Polaron energy branches as a function of axial electric field at $D = 9$ nm.

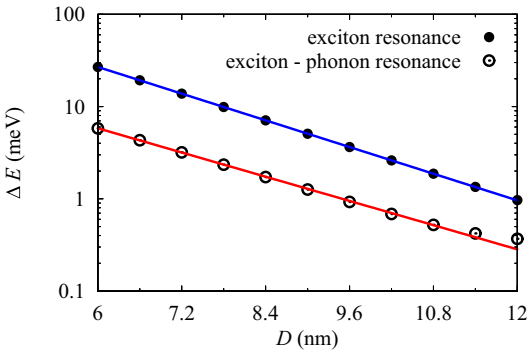

FIG. 4. The width of avoided crossings related to electron tunneling as a function of the interdot distance (E1 in Fig. 2 and box 1 in Fig. 3). The blue/red line corresponds to an exponential fit of the numerical results.

and two-phonon states. The overview of the polaron spectrum, presented in Fig. 3, has been obtained using the minimal basis of s-shell electron and hole states and up to two LO phonons (neglecting two-phonon states would result in the appearance of nonphysical resonances in the single-phonon spectra). In the following discussion, the number of electron states will be extended when needed, while the accuracy of the two-phonon cutoff is justified in the Appendix. We calculated the amplitudes of these components and marked the dominating one in Fig. 3 by assigning colors to the lines: red, green, and blue, respectively. The colors are mixed at the resonances involving states with different numbers of phonons. The central part of the plot corresponds to the states with a dominant zero-phonon (pure excitonic) component. They show the same level structure as in Fig. 2 with only a small shift. The same pattern is reflected in n-phonon replicas at the energies shifted by approximately $n\hbar\Omega$. Box 1 contains an avoided level crossing between the direct exciton state (localized in the upper dot) and the single-phonon replica of the indirect exciton state (the hole in the upper dot and the electron in the lower dot). Thus, this anticrossing corresponds to the resonant electron tunneling combined with emission/absorption of a single LO phonon (decoupled phonon modes do not lead to an anticrossing). The accuracy of the spectrum in the area of this resonance, obtained in the s-shell basis, can be verified by comparison to numerical results performed in an extended basis. We have found that adding electron p- and d-shell states changes the width of this particular resonance by less than 1% and its position just about 0.1 kV/cm.

A similar resonance structure appears for the hole (box 2). However, for the considered DQD, its coupling strength is much weaker than in the electron case. Furthermore, in contrast to the electron case (which already converges in a small basis), the accurate treatment of the hole-phonon resonances would require larger basis which rapidly increases the computation cost. Therefore, we limit our present discussion to the most pronounced electron-phonon resonances. The resonances marked by the box 3 involve the coupling to two-phonon states. They occur at very large electric fields and represent a second-order process with much weaker coupling strength compared to the single-phonon case. Furthermore, a proper treatment of two-phonon states requires taking into account three-phonon states [6].

An interesting question is the dependence of the tunnel coupling strength (extracted from the numerical results as the half-width of the resonant splitting) on the interdot distance. The well-known one-dimensional model of tunneling yields exponential dependence. Such a behavior is indeed obtained for an electron in a DQD structure [34] (which is not obvious, as demonstrated by the hole-related counterexample [35,36]). Therefore, we have investigated the width of the electron tunneling resonance as a function of the distance D between the dots. In Fig. 4, the upper dependence (blue line) corresponds to the electron avoided crossing width (E2 in Fig. 2). The dependence follows the exponential law [37]. We obtained an excellent fit for $f(D) = a\exp(-bD)$ with $a = 0.751$ eV and $b = 0.555$ eV/nm. Similarly to the direct tunnel resonance, we obtained also an exponential decay of the avoided crossing width combined with emission/absorption

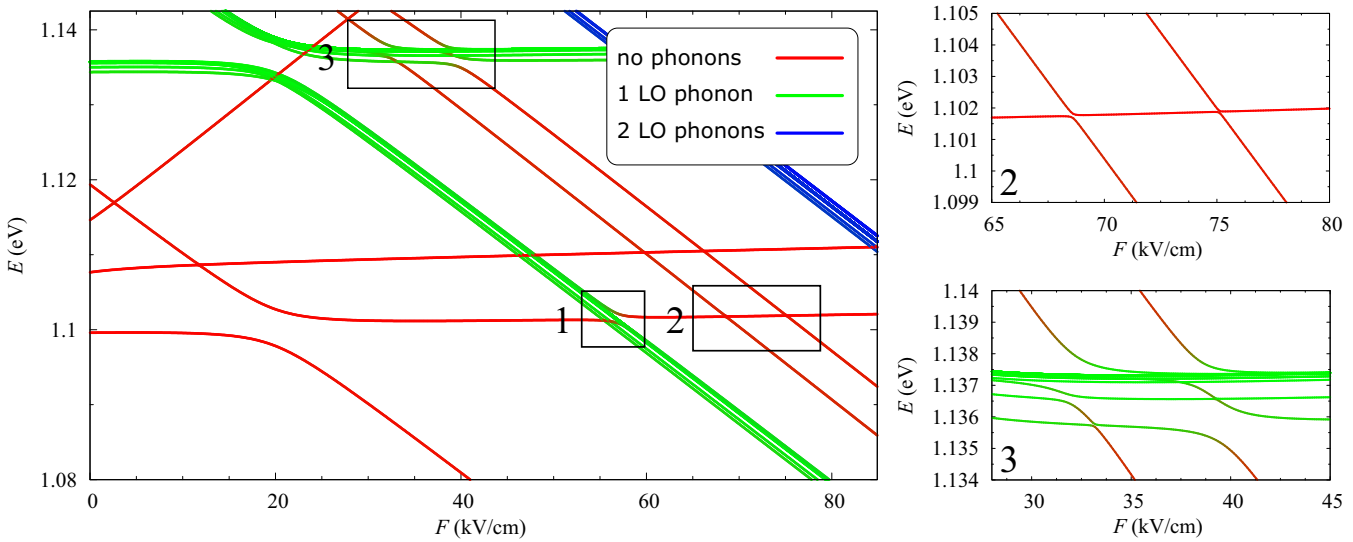

FIG. 5. Polaron energy branches as a function of axial electric field at $D = 9$ nm. The panels on the right show magnified pictures of the corresponding regions.

of LO phonon (corresponding to the box 1 in Fig. 5). The exponential fitting by the function $f(D) = a\exp(-bD)$ yields $a = 0.119$ eV and $b = 0.503\,\mathrm{eV/nm}$. Apart from the much lower amplitude, which is expected for a phonon-assisted process, the decay rate b of the polaron resonance is about 10% lower in comparison to the direct resonance.

In the next step, we study the coupling between the electron p-shell states located in the upper dot and the phonon replica of the s state from the lower one. To this end, we extended the electron basis to 24 states (s, p, d shells in each dot) while the hole basis still contains four states. The results are shown in Fig. 5. The basis extension increases the number of orthogonal phonon modes. The box 2 contains avoided crossing related to the resonant transition between s and p states of the different dots. Since the angular momentum has to be conserved, this coupling is possible only if the axial symmetry of the system is broken. This can be caused, e.g., by the relative displacement of the dots [27], bulk inversion asymmetry (BIA) [38], or emerge from the atomistic structure [39,40]. However, in the present model we assume perfectly aligned dots and the only coupling mechanism is due to BIA and spin-orbit coupling via composition inhomogeneity at the interface. This leads to narrow avoided crossings visible in box 2. On the other hand, phonons carry angular momentum and can couple states with different values of the angular momentum. In consequence, we observe the pronounced anticrossings between the electron states from p shell and the phonon replicas of the s-shell states (see box 3). This LO-phonon-assisted coupling is much stronger than those resulting from BIA (box 2).

IV. SUMMARY

We calculated polaron states for excitons in self-assembled double quantum dots using realistic wave functions obtained from $\boldsymbol{k}\cdot\boldsymbol{p}$ and configuration-interaction calculations. We applied a mode orthogonalization scheme that yields a spanning set of effectively coupled collective modes. We investigated resonances (avoided level crossings) related to the electron resonant tunneling combined with emission/absorption of an LO phonon. We have found that the strength of this LO-phonon-mediated coupling shows exponential dependence on the interdot distance, like in the one-dimensional tunneling problem, with a characteristic length comparable to the direct (zero-phonon) tunneling resonance but with a smaller amplitude. We have also shown that LO-phonon modes can efficiently couple states that belong to different shells (s and p) from different dots. In this case, direct resonance is strongly suppressed by angular momentum selection rules, while the LO-phonon-assisted coupling is allowed and has a larger amplitude.

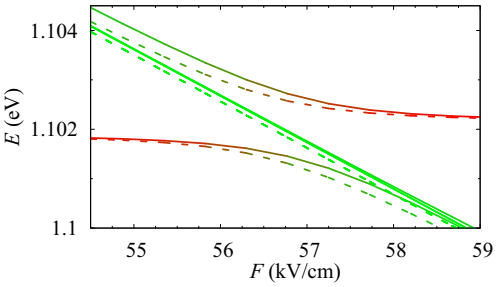

FIG. 6. Comparison of the spectrum around the s-s (box 1 in Fig. 5) resonance as obtained from the model with the basis extended to include three-LO-phonon configurations (dashed lines) and from the two-LO-phonon model, as used in the main body of the paper (solid lines). Color coding as in Figs. 3 and 5.

ACKNOWLEDGMENTS

P.K. acknowledges support by the Grant No. 2014/12/T/ST3/00231 from the Polish National Science Centre (Narodowe Centrum Nauki). K.G. acknowledges support by the Grant No. 2012/05/N/ST3/03079 from the Polish National Science Centre (Narodowe Centrum Nauki). Calculations have been carried out in Wroclaw Centre for Networking and Supercomputing (http://www.wcss.wroc.pl), Grant No. 203.

APPENDIX : THREE-PHONON CORRECTIONS

In this appendix, we present the spectrum around the s-s resonance in a model in order to justify the truncation of our computational basis to at most two-LO-phonon configurations.

The part of the spectrum around the resonance, calculated using a model with s-shell states only but including configurations with up to three LO phonons, is shown in Fig. 6 (dashed lines) and compared to the results from the two-LO-phonon model (solid lines). As one can see, the polaron resonance not only remains qualitatively the same but even quantitatively its width is almost unchanged (it increases by 0,69% only). The position of the resonance is shifted noticeably (by 0.33 kV/cm) but also this shift is small compared to the overall range of the spectrum (tens of kV/cm) and does not affect the physical picture emerging from our results.

[1] N. Zhuo, F. Q. Liu, J. C. Zhang, L. J. Wang, J. Q. Liu, S. Q. Zhai, and Z. G. Wang, Nanoscale Res. Lett. **9**, 144 (2014).
[2] T. Czerniuk, D. Wigger, A. V. Akimov, C. Schneider, M. Kamp, S. Höfling, D. R. Yakovlev, T. Kuhn, D. E. Reiter, and M. Bayer, Phys. Rev. Lett. **118**, 133901 (2017).
[3] R. D. Schaller and V. I. Klimov, Phys. Rev. Lett. **92**, 186601 (2004).
[4] S. Hameau, Y. Guldner, O. Verzelen, R. Ferreira, G. Bastard, J. Zeman, A. Lemaître, and J. M. Gérard, Phys. Rev. Lett. **83**, 4152 (1999).
[5] S. Hameau, J. N. Isaia, Y. Guldner, E. Deleporte, O. Verzelen, R. Ferreira, G. Bastard, J. Zeman, and J. M. Gérard, Phys. Rev. B **65**, 085316 (2002).
[6] P. Kaczmarkiewicz and P. Machnikowski, Phys. Rev. B **81**, 115317 (2010).
[7] T. Stauber, R. Zimmermann, and H. Castella, Phys. Rev. B **62**, 7336 (2000).
[8] O. Verzelen, R. Ferreira, and G. Bastard, Phys. Rev. Lett. **88**, 146803 (2002).
[9] D. E. Reiter, D. Wigger, V. M. Axt, and T. Kuhn, Phys. Rev. B **84**, 195327 (2011).

[10] O. Verzelen, R. Ferreira, and G. Bastard, Phys. Rev. B **62**, R4809 (2000).
[11] L. Jacak, J. Krasnyj, D. Jacak, and P. Machnikowski, Phys. Rev. B **65**, 113305 (2002).
[12] O. Verzelen, G. Bastard, and R. Ferreira, Phys. Rev. B **66**, 081308(R) (2002).
[13] E. A. Zibik, L. R. Wilson, R. P. Green, G. Bastard, R. Ferreira, P. J. Phillips, D. A. Carder, J.-P. R. Wells, J. W. Cockburn, M. S. Skolnick, M. J. Steer, and M. Hopkinson, Phys. Rev. B **70**, 161305(R) (2004).
[14] E. A. Zibik, T. Grange, B. A. Carpenter, N. E. Porter, R. Ferreira, G. Bastard, D. S. S. Winnerl, M. Helm, H. Y. Liu, M. S. Skolnick, and L. R. Wilson, Nat. Mater. **8**, 803 (2009).
[15] B. Szafran, T. Chwiej, F. M. Peeters, S. Bednarek, J. Adamowski, and B. Partoens, Phys. Rev. B **71**, 205316 (2005).
[16] B. Szafran, Acta Phys. Pol. A **114**, 1013 (2008).
[17] H. J. Krenner, M. Sabathil, E. C. Clark, A. Kress, D. Schuh, M. Bichler, G. Abstreiter, and J. J. Finley, Phys. Rev. Lett. **94**, 057402 (2005).
[18] A. S. Bracker, M. Scheibner, M. F. Doty, E. A. Stinaff, I. V. Ponomarev, J. C. Kim, L. J. Whitman, T. L. Reinecke, and D. Gammon, Appl. Phys. Lett. **89**, 233110 (2006).
[19] K. Müller, A. Bechtold, C. Ruppert, M. Zecherle, G. Reithmaier, M. Bichler, H. J. Krenner, G. Abstreiter, A. W. Holleitner, J. M. Villas-Boas, M. Betz, and J. J. Finley, Phys. Rev. Lett. **108**, 197402 (2012).
[20] P.-L. Ardelt, K. Gawarecki, K. Müller, A. M. Waeber, A. Bechtold, K. Oberhofer, J. M. Daniels, F. Klotz, M. Bichler, T. Kuhn, H. J. Krenner, P. Machnikowski, and J. J. Finley, Phys. Rev. Lett. **116**, 077401 (2016).
[21] C. Pryor, J. Kim, L. W. Wang, A. J. Williamson, and A. Zunger, J. Appl. Phys. **83**, 2548 (1998).
[22] D. J. Rowe, J. Math. Phys. **10**, 1774 (1969).
[23] J. S. Blakemore, J. Appl. Phys. **53**, R123 (1982).
[24] J. M. Daniels, P. Machnikowski, and T. Kuhn, Phys. Rev. B **88**, 205307 (2013).
[25] G. Bester, A. Zunger, X. Wu, and D. Vanderbilt, Phys. Rev. B **74**, 081305 (2006).
[26] M. A. Caro, S. Schulz, and E. P. O'Reilly, Phys. Rev. B **91**, 075203 (2015).
[27] K. Gawarecki, P. Machnikowski, and T. Kuhn, Phys. Rev. B **90**, 085437 (2014).
[28] J. Andrzejewski, G. Sęk, E. O'Reilly, A. Fiore, and J. Misiewicz, J. Appl. Phys. **107**, 073509 (2010).
[29] I. Vurgaftman, J. R. Meyer, and L. R. Ram-Mohan, J. Appl. Phys. **89**, 5815 (2001).
[30] M. Świderski and M. Zieliński, Acta Phys. Pol. A **129**, A-79 (2016).
[31] S. Ritter, P. Gartner, N. Baer, and F. Jahnke, Phys. Rev. B **76**, 165302 (2007).
[32] D. Obreschkow, F. Michelini, S. Dalessi, E. Kapon, and M.-A. Dupertuis, Phys. Rev. B **76**, 035329 (2007).
[33] P. Löwdin, J. Chem. Phys. **18**, 365 (1950).
[34] K. Gawarecki, M. Pochwała, A. Grodecka-Grad, and P. Machnikowski, Phys. Rev. B **81**, 245312 (2010).
[35] W. Jaskólski and M. Zieliński, Acta Phys. Pol. A **106**, 193 (2004).
[36] W. Jaskolski, M. Zielinski, G. W. Bryant, and J. Aizpurua, Phys. Rev. B **74**, 195339 (2006).
[37] M. Bayer, G. Ortner, O. Stern, A. Kuther, A. A. Gorbunov, A. Forchel, P. Hawrylak, S. Fafard, K. Hinzer, T. L. Reinecke, S. N. Walck, J. P. Reithmaier, F. Klopf, and F. Schäfer, Phys. Rev. B **65**, 195315 (2002).
[38] R. Winkler, *Spin-Orbit Coupling Effects in Two-Dimensional Electron and Hole Systems*, Vol. 191 of *Springer Tracts in Modern Physics* (Springer, Berlin, 2003).
[39] G. Bester and A. Zunger, Phys. Rev. B **71**, 045318 (2005).
[40] M. Zieliński, Y. Don, and D. Gershoni, Phys. Rev. B **91**, 085403 (2015).